ELSEVIER

Volume 184, Issue 9, September 2011

JOURNAL OF SOLID STATE CHEMISTRY

www.elsevier.com/locate/jssc

# CONTENTS

Abstracted/indexed in BioEngineering Abstracts, Chemical Abstracts, Coal Abstracts, Current Contents/Physics, Chemical, & Earth Sciences, Engineering Index, Research Alert, SCISEARCH, Science Abstracts, and Science Citation Index. Also covered in the abstract and citation database SCOPUS®. Full text available on ScienceDirect®.

## *Regular Articles*



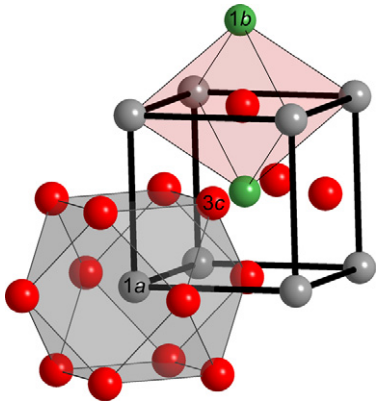


The crystal structure of $GaFe_3N$ with green nitrogen atoms in the very center, red iron atoms at the face centers, and gray gallium atoms at the corner positions.



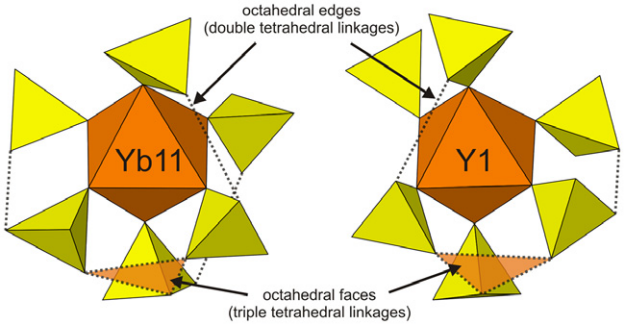


Octahedral-tetrahedral linkages found in $Y_2(SO_4)_3$ [and $Er_2(SO_4)_3$] and ß-$Yb_2(SO_4)_3$.

## *Regular Articles—Continued*



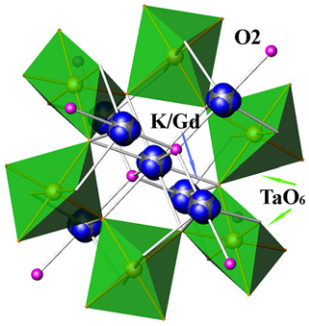


In the pyrochlore tantalate, K and Gd co-occupy the 16*d* site and Ta is on the 16*c* site and forming octahedra with nearby anions. The pyrochlore tantalate is quite resistant to high pressure even when the structure is partially amorphized.



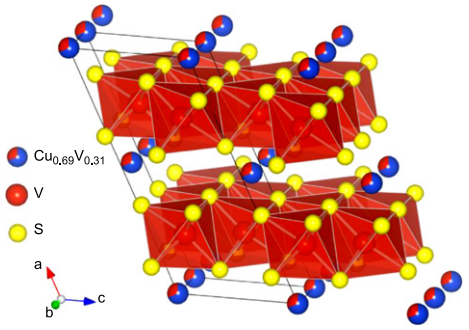


Crystallographic structure of $(Cu_{0.69}V_{0.31})V_2S_4$. For clarity, the octahedral environment of $(Cu_{0.69}V_{0.31})$ site is not shown.

*Continued*

**Fabrication of Cu–Ag core–shell bimetallic superfine powders by eco-friendly reagents and structures characterization**
Jun Zhao, Dongming Zhang and Jie Zhao
***page 2339***

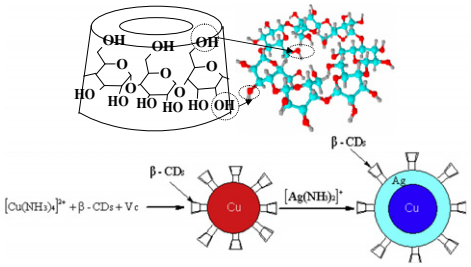


Mechanism of fabricating Cu–Ag particles with good dispersibility using β-CDs as a protective agent was studied because of its special structure.

---

**XAS/EXAFS studies of Ge nanoparticles produced by reaction between $Mg_2Ge$ and $GeCl_4$**
Andrew J. Pugsley, Craig L. Bull, Andrea Sella, Gopinathan Sankar and Paul F. McMillan
***page 2345***

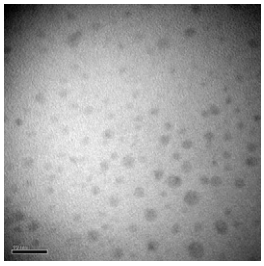

*Nano*-Ge particles 2–10 nm in diameter were prepared by reaction between $Mg_2Ge$ Zintl phase and $GeCl_4$ in diglyme followed by capping with BuLi and extraction into hexane. We used synchrotron X-ray absorption spectroscopy (XAS) at the Ge K edge with analysis of the EXAFS region combined with room temperature photoluminescence and TEM to characterise the nature of the nanoparticles and model compounds and to follow the course of the reaction. A TEM image of the germanium nanoparticles is shown.

---

**Effect of Cr and Mn ions on the structure and magnetic properties of $GaFeO_3$: Role of the substitution site**
Rana Saha, Ajmala Shireen, Sharmila N. Shirodkar, Umesh V. Waghmare, A. Sundaresan and C.N.R. Rao
***page 2353***

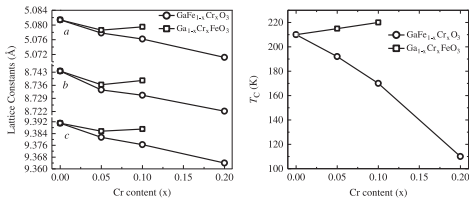


The important role of site-specific substitution of transition metal ions on the structure and magnetic properties of $GaFeO_3$ has been investigated experimentally and theoretically.

---

**Ternary rare-earth zinc arsenides $RE Zn_{1-x}As_2$ ($RE$ = La–Nd, Sm)**
Stanislav S. Stoyko and Arthur Mar
***page 2360***

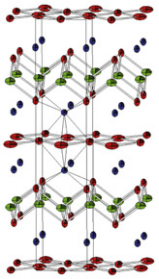

$LaZn_{1-x}As_2$ adopts a $SrZnBi_2$-type structure whereas the remaining members of the $RE Zn_{1-x}As_2$ series ($RE$ = Ce–Nd, Sm) adopt a $HfCuSi_2$-type structure.

---

**Pillared and open-framework uranyl diphosphonates**
Pius O. Adelani and Thomas E. Albrecht-Schmitt
***page 2368***

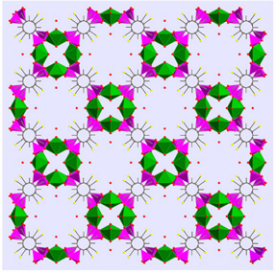

Illustration of the three-dimensional open-framework structure of $\{(UO_2)[C_6H_2F_2(PO_2OH)_2(H_2O)\}_2 \cdot H_2O$ viewed along the $c$-axis. The structure is constructed from $UO_7$ units, pentagonal bipyramids = green, oxygen = red, phosphorus = magenta, carbon = black, hydrogen = white.

---

**Structural and magnetic study of $RFe_{0.5}V_{0.5}O_3$ ($R$ = Y, Eu, Nd, La) perovskite compounds**
M. Gateshki, L. Suescun, S. Kolesnik, J. Mais and B. Dabrowski
***page 2374***

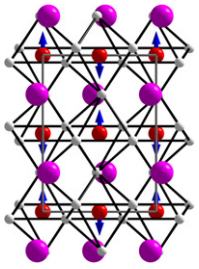

$G_z$ type antiferromagnetic ordering of Fe and V moments in B-site disordered $RFe_{0.5}V_{0.5}O_3$ perovskites ($R$ = La, Nd, Y) with $a^+b^-b^-$ octahedral tilt and orthorhombic (*Pbnm* space group) structure determined by neutron powder diffraction.

**Raman scattering from La-substituted $BiFeO_3$–$PbTiO_3$**
K.K. Mishra, V. Sivasubramanian, R.M. Sarguna, T.R. Ravindran and A.K. Arora
***page 2381***

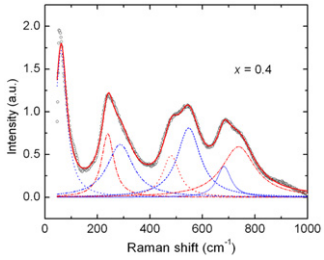


Raman spectrum of the cubic phase ($x \geq 0.4$) of La-substituted BF–PT [$0.5(Bi_{1-x}La_xFeO_3)0.5(PbTiO_3)$] consists of 7 modes, while group theory does not predict any Raman active phonon.

---

**The electronic structure of the $CuRh_{1-x}Mg_xO_2$ thermoelectric materials: An X-ray photoelectron spectroscopy study**
T.K. Le, D. Flahaut, H. Martinez, N. Andreu, D. Gonbeau, E. Pachoud, D. Pelloquin and A. Maignan
***page 2387***

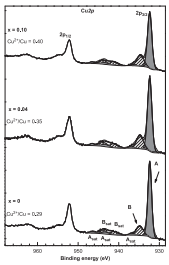

The role of the Mg substitution in the $CuRh_{1-x}Mg_xO_2$ as a function of $x$ ($x = 0$, 0.04 and 0.1) has been investigated by following the evolution of the Cu2*p* spectra obtained by X-ray photoelectron spectroscopy. The filled peaks are assigned to main peak *A* and $A_{sat}$ satellites, the hatched peaks to main peak *B* and $B_{sat}$ satellites.

---

**Preparation and characterization of novel alkylviologens-intercalated vanadyl-vanadate (*RV*)$V_3O_8$**
Keqiang Lai, Aiguo Kong, Yongjie Ding, Hengqiang Zhang and Yongkui Shan
***page 2393***

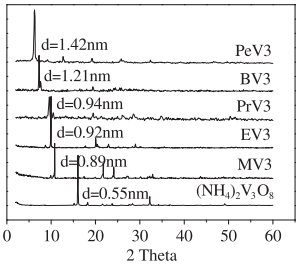


The (001) reflection of the intercalation compounds shifting to a lower $2\theta$ value in comparison with that of $(NH_4)_2V_3O_8$ implies the interlayer space was undergone expansion after intercalation.

**A new ordered triple Hollandite: $Ba_{1.33}Sb_{2.66}Al_{5.33}O_{16}$**
A. Letrouit, S. Boudin, N. Barrier and R. Retoux
***page 2398***

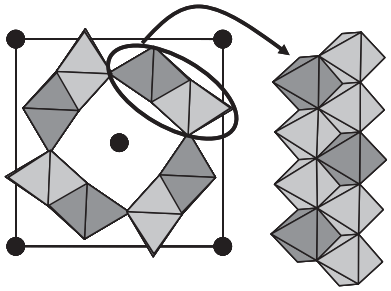

The new $Ba_{1.33}Sb_{2.66}Al_{5.33}O_{16}$ triple Hollandite has been synthesized and characterized by X-ray diffraction, electron microscopy, and cyclic voltammetry.

---

**Self-assembly of $Fe_3O_4$ nanocrystal-clusters into cauliflower-like architectures: Synthesis and characterization**
Lu-Ping Zhu, Gui-Hong Liao, Nai-Ci Bing, Lin-Lin Wang and Hong-Yong Xie
***page 2405***

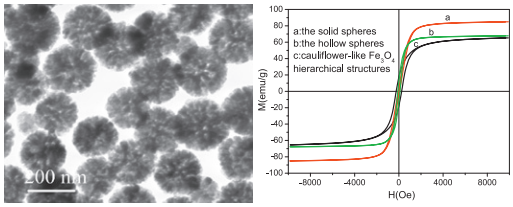


Cauliflower-like $Fe_3O_4$ architectures consist of well-assembled magnetite nanocrystal clusters have been synthesized by a simple solvothermal process, using $FeCl_3 \cdot 6H_2O$ and EDA as the starting materials.

---

**Structural originations of irreversible capacity loss from highly lithiated copper oxides**
Corey T. Love, Wojtek Dmowski, Michelle D. Johannes and Karen E. Swider-Lyons
***page 2412***

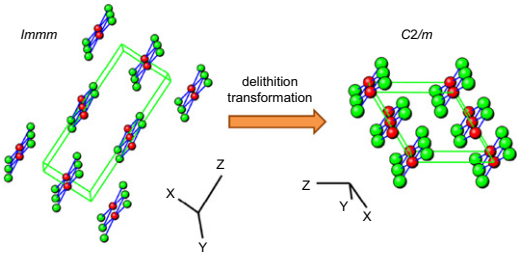


Structural transformation from $Li_2CuO_2$ to delithiated $LiCuO_2$.

*Continued*

**Stepwise synthesis, characterization, and electrochemical properties of ordered mesoporous carbons containing well-dispersed Pt nanoparticles using a functionalized template route**

Shou-Heng Liu and Shih-Che Chen

*page 2420*

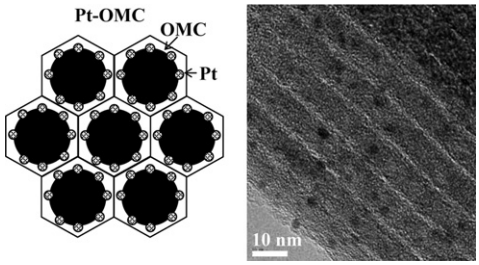


A novel procedure has been developed to synthesize ordered carbon mesoporous carbons (OMC) containing well-dispersed and highly electrocatalytic Pt nanoparticles (Pt–OMC) for oxygen reduction reaction.

---

**Structural and magnetic characterization of $BiFe_xMn_{2-x}O_5$ oxides ($x = 0.5$, 1.0)**

M. Retuerto, M.J. Martínez-Lope, K. Krezhov, M.T. Fernández-Díaz and J.A. Alonso

*page 2428*

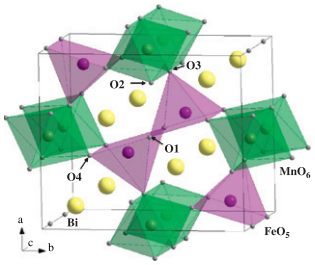


$BiFe_xMn_{2-x}O_5$ ($x = 0.5$, 1.0) samples are isostructural with $BiMn_2O_5$, belonging to the *Pbam* space group. The crystal structure contains infinite chains of edge-sharing $Mn^{4+}O_6$ octahedra, interconnected by dimer units of $Fe^{3+}O_5$ square pyramids. These units are strongly distorted due to the presence of the electronic lone pair on $Bi^{3+}$. They are magnetically ordered at low temperatures. The main magnetic interactions seem to be antiferromagnetic with the presence of some weak ferromagnetic response.

---

**The crystal and magnetic structure of the magnetocaloric compound $FeMnP_{0.5}Si_{0.5}$**

Viktor Höglin, Matthias Hudl, Martin Sahlberg, Per Nordblad, Premysl Beran and Yvonne Andersson

*page 2434*

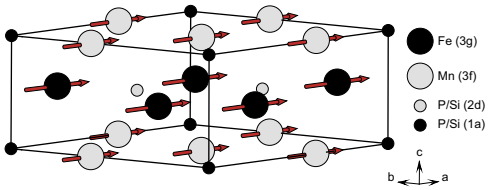


The magnetic structure of $FeMnP_{0.5}Si_{0.5}$ at 296 K. Revealed from refinements of neutron powder diffraction data.

**Methotrexate intercalated ZnAl-layered double hydroxide**

Manjusha Chakraborty, Sudip Dasgupta, Chidambaram Soundrapandian, Jui Chakraborty, Swapankumar Ghosh, Manoj K. Mitra and Debabrata Basu

*page 2439*

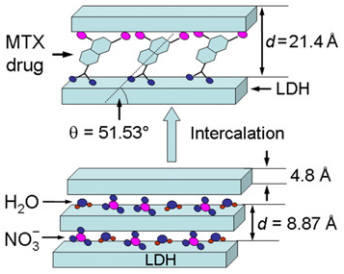


ZnAl-layered double hydroxide intercalated with methotrexate (~34% loading) promises the possibility of use of ZnAl-LDH material as drug carrier and in controlled delivery.

---

**Phonon properties of nanosized $MnWO_4$ with different size and morphology**

Mirosław Mączka, Maciej Ptak, Michalina Kurnatowska, Leszek Kępiński, Paweł Tomaszewski and Jerzy Hanuza

*page 2446*

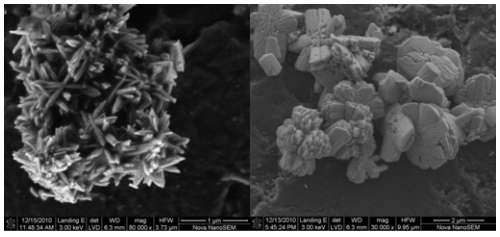

SEM images of $MnWO_4$ particles prepared by hydrothermal process at 150 °C (left panel) and 200 °C (right panel).

---

**Two types of diffusions at the cathode/electrolyte interface in IT-SOFCs**

Zhi-Peng Li, Toshiyuki Mori, Graeme John Auchterlonie, Jin Zou and John Drennan

*page 2458*

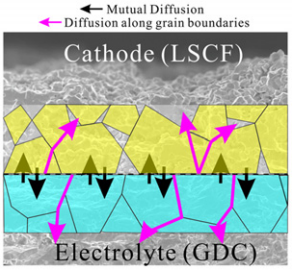


Two types of diffusions, the mutual diffusion and the diffusion along grain boundaries, occurred at the cathode/electrolyte interface of intermediate temperature solid state fuel cells, during cell preparation. The mutual diffusion is denoted by black arrows and the diffusion along grain boundaries assigned by pink arrows.

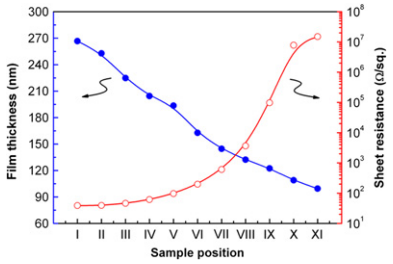


The film thickness and the sheet resistance ($R_s$) with respect to the sample position of WInZnO films, which is compositionally graded by rf power for each target, are exhibited.



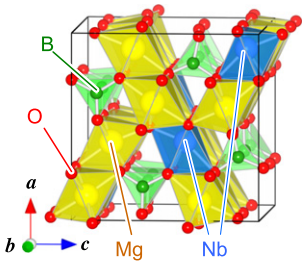


Single crystals of new oxyborates, $Mg_5NbO_3(BO_3)_3$ and $Mg_5TaO_3(BO_3)_3$, were synthesized by a self flux method. They crystallize in novel warwickite-type superstructures having ordered arrangements of Mg and Nb/Ta atoms.



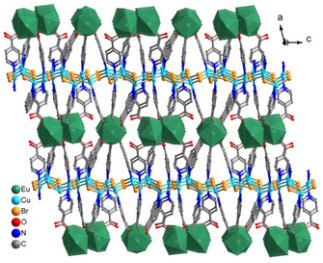

Two unusual pillared-layer Eu (Gd)–Cu heterometallic coordination polymers have been hydrothermally synthesized. The luminescent properties of Eu–Cu compound and magnetic properties of both compounds are investigated.



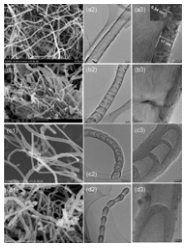

Four types of BN nanotubes are selectively synthesized by annealing porous precursor prepared by self-propagation high-temperature synthesis. Three phenomenological growth models are proposed to reveal growth scenario and characteristics of the as-synthesized BN nanotubes.



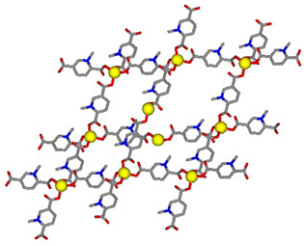

Reaction of $Zn(NO_3)_2 \cdot 6H_2O$ with a deliberately designed unsymmetrical ligand 2.5-dicarboxy-1-methylpyridinium (DCMP) chloride and in the presence of $NaHCO_3$ gave an expected noncentric diamondoid network $[Zn(DCMP)_2]$, which has its SHG response approximately 7 times higher than that of potassium dihydrogen phosphate (KDP).



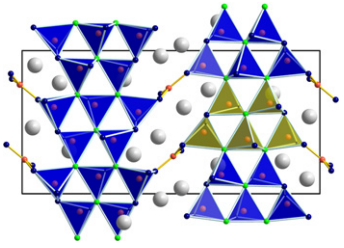

The new high-pressure compound HP-$LiB_3O_5$ is built up from a three-dimensional network of BO4 tetrahedra and $BO_3$ groups, which incorporates $Li^+$ ions in channels along the *b*-axis. In this paper, the synthesis, the crystal structure, and the properties of HP-$LiB_3O_5$ are described.

*Continued*

**Structural and physical properties of the new intermetallic compound $Yb_3Pd_2Sn_2$**

P. Solokha, I. Čurlik, M. Giovannini, N.R. Lee-Hone, M. Reiffers, D.H. Ryan and A. Saccone

*page 2498*

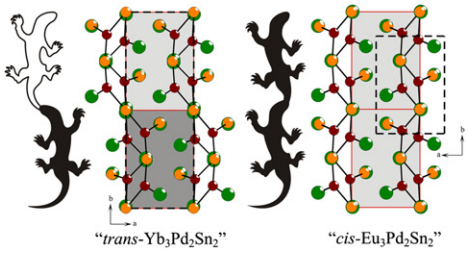


Polyanionic networks for $Yb_3Pd_2Sn_2$ and $Eu_3Pd_2Sn_2$.

---

**Two new zincophosphates, $(H_3NCH_2CH_2NH_3)_2[Zn(\mu\text{-}PO_4)_2]$ and $(NH_4)[(H_3N)Zn\{(\mu\text{-}PO_4)Zn\}_3]$: Crystal structures and relationships to similar open framework zinco- and aluminophospates**

Ljiljana Karanović, Dejan Poleti, Tamara Đorđević and Sabina Šutović

*page 2506*

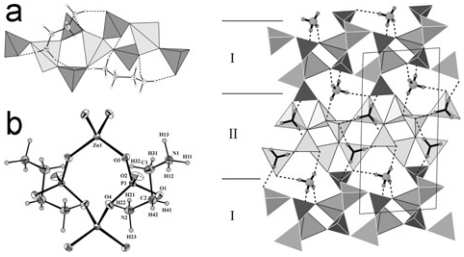


Structure of **1** (left): polyhedral (a) and ORTEP-like (b) representation of the $ZnP_2O_8^{4-}$ chain with two $H_2en^{2+}$ cations. Structure of **2** (right): polyhedral structure of the layers I and II seen along [1 0 0] (*c*-axis is vertical).

---

**Local deuterium order in apparently disordered Laves phase deuteride $YFe_2D_{4.2}$**

J. Ropka, R. Černý and V. Paul-Boncour

*page 2516*

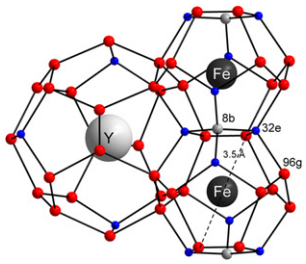


Deuterium short-range order in cubic Laves phase deuteride $YFe_2D_{4.2}$ was studied by *ToF* neutron powder diffraction experiments and Pair Distribution Function analysis between 290 and 400 K. It has been found that the distribution of deuterium atoms around the iron is not random, and cannot be explained only by applying the Switendick rule. The first coordination sphere of iron atoms in the HT-disordered phase resembles that of the LT-ordered phase.

**Phase composition and magnetic properties of niobium–iron codoped $TiO_2$ nanoparticles synthesized in $Ar/O_2$ radio-frequency thermal plasma**

Chenning Zhang, Masashi Ikeda, Masaaki Isobe, Tetsuo Uchikoshi, Ji-Guang Li, Takayuki Watanabe and Takamasa Ishigaki

*page 2525*

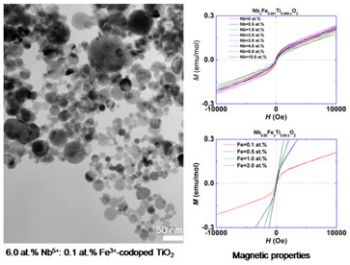


Spherical nanoparticles of $Nb^{5+}$–$Fe^{3+}$ codoped $TiO_2$ were synthesized using $Ar/O_2$ thermal plasma. The plasma-synthesized powders were composed of anatase as major phase and rutile. Rutile weight fraction was increased by $Fe^{3+}$ addition but was reduced by $Nb^{5+}$ doping. Strongly paramagnetic and feebly ferromagnetic properties are of intrinsic nature. Ferromagnetic properties gradually deteriorated as $Fe^{3+}$ concentration was increased.

---

**Crystal structure of Eu-doped magnetoplumbite-type lanthanum aluminum oxynitride with emission site splitting**

Yuji Masubuchi, Tomoyuki Hata, Teruki Motohashi and Shinichi Kikkawa

*page 2533*

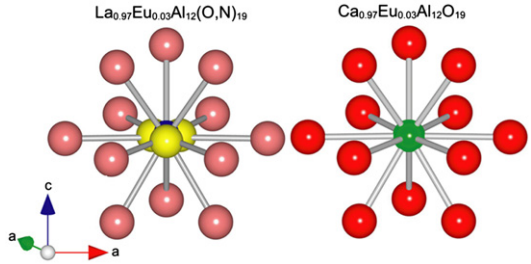


Magnetoplumbite type Eu-doped lanthanum aluminum oxynitride has lanthanum site splitting induced by two kinds of anions, causing two emission peaks.

---

**A new organically-templated cobalt borophosphate with a novel borophosphatic anionic partial structure**

Wei Liu, Xiang-Qin Guo, Ge Su, Li-Xin Cao, Yong-Gang Wang and Jing-Rui Duan

*page 2538*

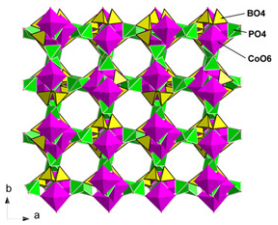


A new organically-templated cobalt borophosphate, $(NH_4)_2(C_4H_{12}N_2)[Co_2B_4P_6O_{24}(OH)_2]\cdot H_2O$ with a novel borophosphate 3D anionic partial framework has been synthesized under mild hydrothermal conditions.

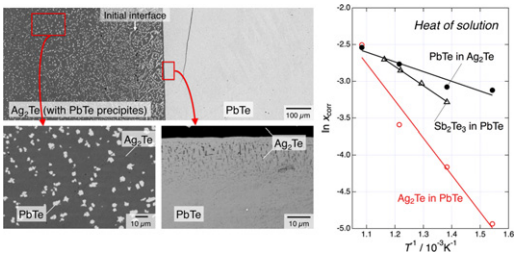


The precipitation in the diffusion couple in fast cooling suggests high chemical diffusivity. The large heat of solution for the $Ag_2$ Te dissolution in PbTe leads to fine microstructure.



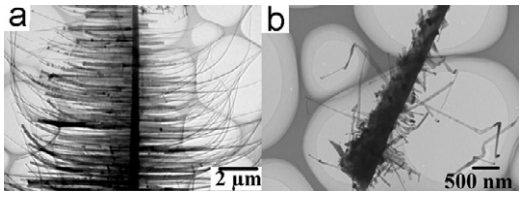


Spine-shaped and pine-shaped $Si_3N_4$ hierarchical nanostructures were synthesized by VS and VLS mode with plasma-assisted dc arc discharge method.



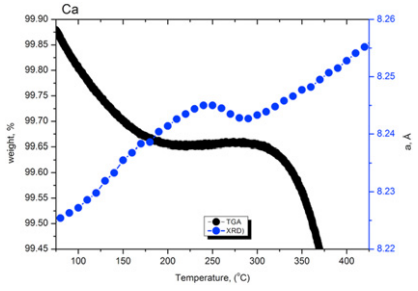


The oxides $Sr_2BSbO_{5.5}$ ($B$ = Ca, Sr, Ba) have unusual anion disorder. There is a lag in the contraction in the cell size of $Sr_2CaSbO_{5.5}nH_2O$ established from X-ray diffraction measurements following the loss of water suggesting changes on the local structure are important.



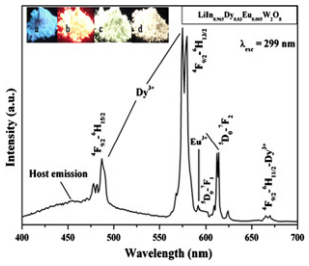


$LiInW_2O_8$:$Eu^{3+}$, $Dy^{3+}$/$Eu^{3+}$ emits red and white colors, respectively, under host excitation wavelength. An effective energy transfer from $LiInW_2O_8$ to $Eu^{3+}$ and $Dy^{3+}$ ions is occurred. $Eu^{3+}$ and $Dy^{3+}$ occupy non-centrosymmetric sites in the host lattice.



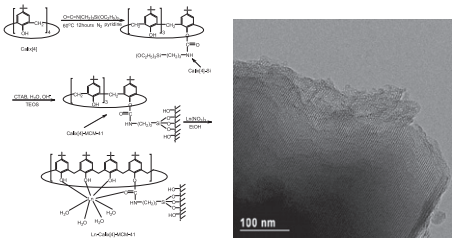


MCM-41 mesoporous silica is functionalized with two kinds of macrocylic calixarene derivatives and luminescent organic–inorganic mesoporous hybrids containing $Ln^{3+}$ complexes covalently attached to the functionalized ordered mesoporous MCM-41.



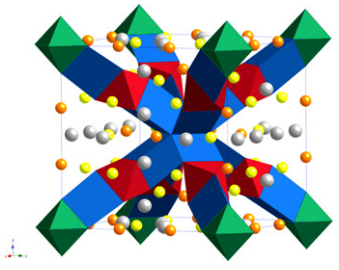

Cation and anion vacancies are found to coexist in mixed-metal oxides that adopt the $La_{18}Li_8Rh_5O_{39}$ structure.

*Continued*

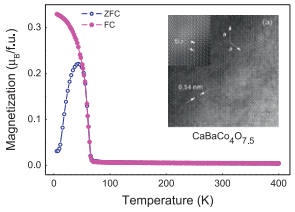


The study of the oxidation of the "114" orthorhombic cobaltite $CaBaCo_4O_7$, using first electrochemistry and then soft chemistry based on oxidation by NaClO, has allowed a new phase, $CaBaCo_4O_{7.50}$, to be prepared topotactically. The structural study of this phase shows that its hexagonal structure, closely related to that of orthorhombic $CaBaCo_4O_7$, is curiously similar to that of the members of the $LnBaCo_4O_7$ series, in spite of its oxygen excess. Its magnetic study shows that this phase, like $CaBaCo_4O_7$, is ferrimagnetic.



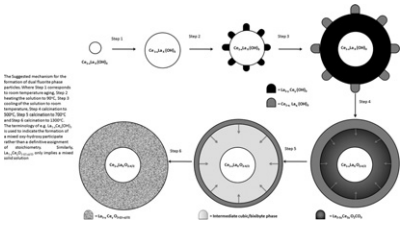

The suggested mechanism for the formation of dual fluorite phase particles, where Step 1 corresponds to room temperature aging, Step 2; heating the solution to 90 °C, Step 3; cooling of the solution to room temperature, Step 4; calcination to 500 °C, Step 5; calcination to 700 °C and Step 6; calcination to 1300 °C. The terminology of e.g. $La_{1-x}Ce_x(OH)_3$ is used to indicate the formation of a mixed oxy-hydroxy participate rather than a definitive assignment of stoichiometry. Similarly, $La_{1-y}Ce_yO_2$ only implies a mixed solid solution .



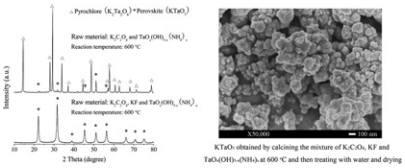

Pyrochlore-free $KTaO_3$ powder was prepared at 600 °C using tantalum hydroxide/$K_2C_2O_4$/KF raw materials. Pyrochlore $K_2Ta_2O_6$ and perovskite $KTaO_3$ coexist at 600 °C using tantalum hydroxide/$K_2C_2O_4$ raw materials.

## *Rapid Communications*



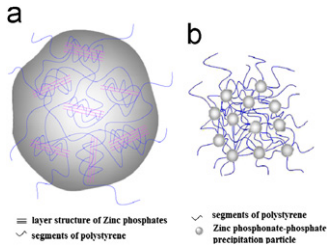


Zinc poly(styrene-phenylvinylphosphonate)-phosphate was a novel type of layered crystalline organic polymer–inorganic hybrid material prepared under mild conditions without addition of any template and could be used as heterogeneous catalyst supports.



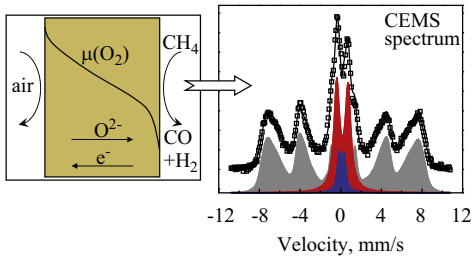


Conversion-electron Mössbauer spectroscopy analysis of dense ceramic membranes made of $^{57}Fe$-enriched $SrFe_{0.7}Al_{0.3}O_{3-\delta}$ perovskite, shows no reductive decomposition in thin interfacial layers after testing under air/$CH_4$ gradient, enabling stable operation of the ferrite-based ceramic reactors for partial oxidation of methane.

## *Corrigendum*

## Author inquiries

For inquiries relating to the submission of articles (including electronic submission where available) please visit this journal's homepage at http://www.elsevier.com/locate/jssc. You can track accepted articles at http://www.elsevier.com/trackarticle and set up e-mail alerts to inform you of when an article's status has changed. Also accessible from here is information on copyright, frequently asked questions and more.
Contact details for questions arising after acceptance of an article, especially those relating to proofs, will be provided by the publisher.

**Language services.** Authors who require information about language editing and copyediting services pre- and post-submission please visit http://www.elsevier.com/locate/languagepolishing or our customer support site at http://epsupport.elsevier.com. Please note Elsevier neither endorses nor takes responsibility for any products, goods or services offered by outside vendors through our services or in any advertising. For more information please refer to our Terms & Conditions http://www.elsevier.com/termsandconditions

For a full and complete Guide for Authors, please go to: http://www.elsevier.com/locate/jssc

*Journal of Solid State Chemistry* has no page charges.